Original Article

Evaluating fetal lung development at various gestational weeks using two-dimensional shear wave elastography

Danyi Liu[1]^, Qiuxia Jiang[2], Ziwei Xu[1], Liya Li[1], Guorong Lyu[1]^

[1]Department of Ultrasound, Second Affiliated Hospital of Fujian Medical University, Quanzhou, China; [2]Department of Ultrasound, Quanzhou Women's and Children's Hospital, Quanzhou, China

Contributions: (I) Conception and design: G Lyu, L Li; (II) Administrative support: G Lyu, Q Jiang; (III) Provision of study materials or patients: D Liu, Q Jiang; (IV) Collection and assembly of data: D Liu, Z Xu; (V) Data analysis and interpretation: D Liu; (VI) Manuscript writing: All authors; (VII) Final approval of manuscript: All authors.

Correspondence to: Guorong Lyu, MD, PhD. Department of Ultrasound, Second Affiliated Hospital of Fujian Medical University, Donghai Street, Fengze District, Quanzhou 362000, China. Email: lgr_feus@sina.com.

Background: Noninvasive evaluation of fetal lung development is a critical area of study. Two-dimensional shear-wave elastography (2D-SWE) provides valuable insights into tissue stiffness, potentially correlating with different stages of lung development. This study aims to explore the potential of the 2D-SWE technique for assessing the maturity of fetal lung development.

Methods: This prospective cohort study included pregnant women undergoing routine antenatal ultrasound examinations at the Second Affiliated Hospital of Fujian Medical University and Quanzhou Women's and Children's Hospital from September 2022 to September 2023. The study consecutively recruited 300 pregnant women with normal pregnancies and 15 who opted for induced labor. Among those with normal pregnancies, the study assessed the differences in fetal pulmonary and hepatic elasticity measurements across different gestational weeks (GW) using one-way analysis of variance (ANOVA). Furthermore, regression analyses using linear, quadratic, and cubic equations were conducted to investigate the relationship between fetal parameters and GW. For those who opted for induced labor, elasticity measurements were taken before induction, and fetal lung tissue specimens were collected for post-induction observation.

Results: Fetal lung and liver elasticity values, along with the lung-to-liver elasticity ratio (LLE ratio), showed significant variations across different GW ($P<0.05$). Specifically, fetal lung elasticity values initially increased and then decreased as GW advanced ($R2=0.41$). Liver elasticity values continuously increased throughout GW, though the rate of increase diminished during the prenatal period ($R2=0.37$). The LLE ratio values increased and then decreased over GW, fluctuating overall between 0.8 and 0.9 ($R2=0.14$). A 71.4% concordance was observed between the predicted stage of lung development, based on lung elasticity values, and the histological stage of lung development in the induced fetuses.

Conclusions: 2D-SWE can depict the maturation of fetal lung development at various stages.

Keywords: Feta; lung; liver; histology; two-dimensional shear-wave elastography (2D-SWE)

Submitted Feb 08, 2024. Accepted for publication Jul 01, 2024. Published online Jul 30, 2024.
doi: 10.21037/qims-24-272
View this article at: https://dx.doi.org/10.21037/qims-24-272

^ ORCID: Danyi Liu, 0009-0006-9290-5692; Guorong Lyu, 0000-0003-3123-1138.

Introduction

Fetal lung development is categorized into five stages: the embryonic period (4–7 weeks), pseudoglandular stage (5–17 weeks), canalicular stage (16–26 weeks), saccular stage (24–38 weeks), and alveolarization (>36 weeks). During the canalicular stage, the initial air-blood barrier forms in the lungs, initiating the production of small amounts of surfactant. In the saccular stage, glandular vesicles progressively elongate and widen, resulting in the formation of a balloon-like structures, which give this phase its name (1). Alveolar development is an extended process, that continues from 36 weeks of gestation until birth. Remarkably, recovery and the formation of new alveoli can occur in exceptional cases, such as in adults when the lungs suffer permanent damage due to bronchopulmonary dysplasia or following pneumonectomy or lobectomy (2,3).

Assessing the degree of fetal lung development is crucial. Given the widespread use of ultrasound for fetal examination, numerous researchers have explored various ultrasound imaging methods to evaluate fetal lung maturity. Two-dimensional (2D) ultrasound can evaluate fetal lung development by measuring biparietal diameters, placental grading, and echoes of the thalamus and intestines (4). Tang *et al.* (5) demonstrated that parameters such as the rapid systolic time of the main pulmonary artery and the ratio of rapid systolic time to ejection time measured by Doppler ultrasound can serve as noninvasive tests for assessing fetal lung development. Khalifa *et al.* (6) utilized three-dimensional ultrasound to record fetal lung volumes, offering an improved assessment of fetal lung development. Nevertheless, the specificity and sensitivity of these methods for determining fetal lung maturity are not highly satisfactory.

Recently, two-dimensional shear wave elastography (2D-SWE) has been extensively used in diagnosing liver fibrosis, thyroid cancer, breast cancer, and various other diseases. Compared to conventional ultrasound, shear wave elastography quantitatively measures tissue stiffness and avoids the measurement bias associated with strain elastography, offering new diagnostic information and expanding its clinical applications (7). However, its application in obstetrics is less common (8-11). This study aimed to establish a reference range of normal values for fetal lung and liver elasticity at different gestational weeks (GW) using 2D-SWE. Historically, liver elasticity values have been used as a reference for comparing stiffness between the two organs (12,13). Mottet *et al.* (14) first proposed the lung-to-liver elasticity ratio (LLE ratio) as a new parameter to reflect changes in both lung and liver elasticity values. Therefore, we included the LLE ratio as a new parameter in this study. Since no studies have linked fetal lung elasticity values to lung tissue sections to assess the reliability of these values in predicting lung development, this study aimed to determine whether fetal lung elasticity values can accurately assess the stage of fetal lung development and to examine fetal lung tissue post-induction of labor. We present this article in accordance with the STROBE reporting checklist (available at https://qims.amegroups.com/article/view/10.21037/qims-24-272/rc).

Methods

Study populations

From September 2022 to September 2023, a prospective observational study was conducted at the Second Affiliated Hospital of Fujian Medical University and Quanzhou Women's and Children's Hospital. The study adhered to the Declaration of Helsinki (revised in 2013). It was approved by the institutional review board of the Second Affiliated Hospital of Fujian Medical University (No. 2022296) and registered at chictr.org.cn (ChiCTR2300077320). Quanzhou Women's and Children's Hospital was also informed and agreed to participate in the study. All pregnant women involved provided informed consent by signing a consent form. The permissible error (δ) was set at 0.3, and the standard deviation (σ) at 0.55, based on the sample size formula $N=\frac{Z^2\sigma^2}{\delta^2}$, resulting in a sample size of approximately 13 per GW. To account for potential attrition, the sample size was increased by about 15%, resulting in a total of 300 pregnant women with normal pregnancies (see *Table 1* for basic information and *Figure 1* for flow chart).

Inclusion criteria for normal pregnant women included: (I) singleton pregnancy; (II) regular and normal menstruation, with early pregnancy ultrasound measurements aligning with GW; (III) routine prenatal ultrasound screening showing no abnormalities; (IV) normal follow-up of the newborn. Exclusion criteria were: (I) twin or multiple pregnancies; (II) pregnant women with systemic diseases such as gestational diabetes mellitus or gestational hypertension; (III) conditions like intrauterine growth restriction or preterm labor affecting fetal growth and development; (IV) malformations or pathologies in the

fetal lungs or liver; (V) detection of fetal malformations during prenatal ultrasound examinations; (VI) use of corticosteroids at any GW prior to the test.

The inclusion criteria for the induced labor group were: (I) pregnant women opting for pregnancy termination between 20–37 GW; (II) obstetricians confirming eligibility for induced labor and proceeding with induction at our hospital. The exclusion criteria were: (I) pregnant women and their families declining lung tissue autopsy on the induced fetus; (II) pregnant women not undergoing 2D-SWE examination within 3 days before induced labor.

Table 1 Maternal and infant characteristics

Characteristics	Values
Maternal characteristics	
Age (years)	30.99±5.27
BMI (kg/m^2)	23.44±1.76
First pregnancy (cases)	132/300 (44.0%)
Obedient births (cases)	187/300 (62.3%)
Infant characteristics	
Male (cases)	157/300 (52.3%)
Gestational age at birth (weeks)	38.67±1.12
Weight (g)	3,219.87±279.69

Quantitative variables are expressed as mean ± standard deviation. Qualitative variables are expressed as proportions with their shares in parentheses. BMI, body mass index.

Research methods

The Mindray Resona R9 diagnostic ultrasound machine (Shenzhen Mindray Biomedical Electronics Co., Ltd., Shenzhen, China), equipped with a 5 MHz abdominal convex array probe utilizing harmonic imaging technology, was employed for this study. Instrument settings were meticulously adjusted to ensure compliance with safety standards: the mechanical index (MI) was <1.9, the thermal index of soft tissue (TIS) was ≤0.7, and the maximum spatial peak time-averaged intensity was <720 mW/cm^2. 2D-SWE was used for measurements, with each session lasting no longer than 10 minutes. Data were obtained from a circular region of interest (ROI) measuring 5 mm in diameter (see *Figure 2* for a schematic illustration). Image acquisition protocols were standardized across all participants, with measurements taken at depths not exceeding 8 cm. Each ROI measurement was repeated three times, and the average value was recorded. The physicians responsible for ultrasound gestational age assessments, elasticity measurements, and lung tissue observations were blinded to each other's findings. All participating physicians had more than three years of experience in their respective specialties and were guided by field experts throughout the study.

Fetal lung development stages were categorized following the methodology proposed by Schittny (1). These stages include the embryonic period (4–7 weeks of gestation), the pseudoglandular stage (5–15 weeks), the transition from pseudoglandular to canalicular stage (16–17 weeks),

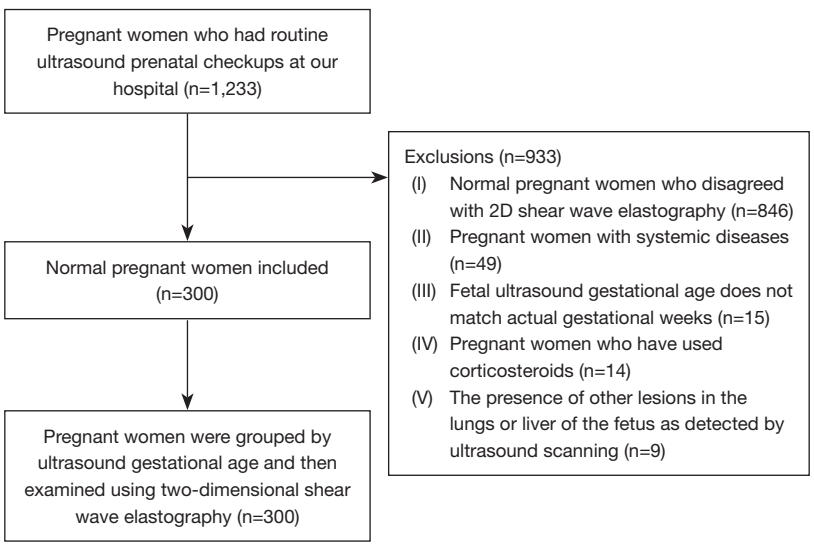

Figure 1 Flowchart for the collection of normal fetal lung and liver elasticity values.

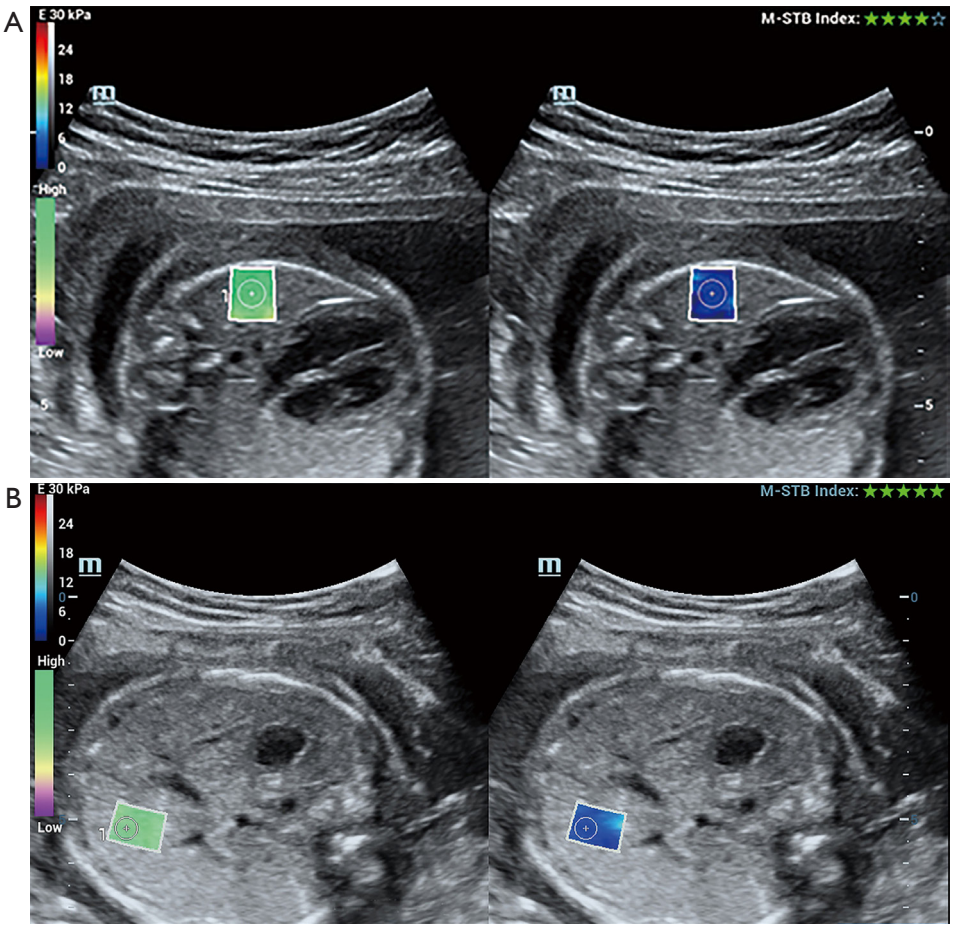

Figure 2 Real-time schematic during the measurement of fetal lung and liver elasticity values. (A) A schematic diagram of lung elasticity value measurements and (B) a schematic diagram of liver elasticity value measurements. All measurements were performed in split-screen mode. Green in the sampling box on the left screen indicates high confidence, while purple color indicates low confidence. Blue in the sampling frame on the right screen indicates soft tissue, and red indicates hard tissue. The region of interest is a circle with a diameter of 5 mm.

the canalicular stage (18–23 weeks), the transition from canalicular to saccular stage (24–26 weeks), the saccular stage (27–35 weeks), the transitional stage from saccular to alveolarization (36–38 weeks), and the alveolarization stage (>36 weeks of gestation).

Within 30 minutes post-abortion, fetal lung tissue specimens were promptly fixed in 10% neutral buffered formalin in a 60 mL disposable specimen container. After a 24-hour fixation period, specimens were dehydrated, embedded, and processed routinely into 4- to 5-micron-thick sections, which were then stained with hematoxylin and eosin. Two physicians independently evaluated sections of lung tissue from each induced fetus, categorizing them into the pseudoglandular, canalicular, saccular, and alveolarization stages, or transitional phases between adjacent stages, based on morphological observations. Both physicians conducted their assessments independently, without access to each other's findings. In case of discrepancy, consensus was reached through mutual consultation between the two physicians.

The developmental stage inferred from fetal lungs elasticity values was compared with the stage determined from microscopic examination of fetal lung tissue. Concordance was noted if both stages matched, whereas discordance indicated differences between them. Fetal lung development was categorized as delayed if histological stage preceded that determined by ultrasound gestational age, as normal if both stages coincided, and as overdue if histological development lagged behind ultrasound assessment (see *Figure 3*).

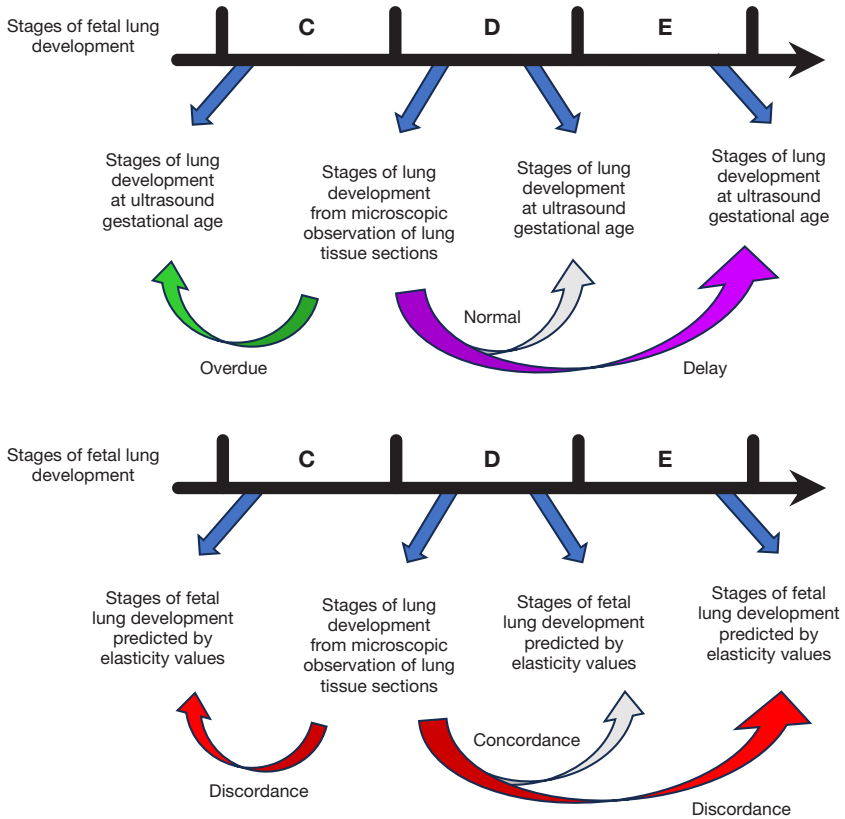

Figure 3 Explanation of the definitions of overdue, normal, delay, discordance, and concordance. C, the canalicular stage; D, the saccular stage; E, the alveolarization.

Statistical methods

Statistical analyses and curve fitting were performed using SPSS 26.0 and GraphPad Prism 9.5.1 software. Normal distribution of measures was assessed using the histogram test, and homogeneity of variances was examined using Levene's test. Normally distributed data were presented as mean ± standard deviation ($\bar{x} \pm s$). Differences among GW were evaluated using one-way analysis of variance (ANOVA). The relationship between fetal measures and GW was explored using regression analysis, including linear, quadratic, and cubic models. Model comparisons led to the selection of the best-fitting equation. Statistical significance was defined as P<0.05 (two-sided).

Results

Fetal lung and liver elasticity values and LLE ratio at different GW

Statistically significant differences were observed in normal fetal lung and liver elasticity values, as well as LLE ratios, across various GW (P<0.05). The detailed data are presented in *Table 2*. *Figure 4* illustrates the trends in normal fetal lung and liver elasticity values, along with LLE ratios, as a function of GW. The quadratic regression equation for fetal pulmonary elasticity values in relation to GW is as follows:

$$E_{lung}(\text{Unit:kPa}) = -1.663 + 0.3920GW - 0.006205GW^2 \left(R^2 = 0.41\right) \quad [1]$$

The quadratic regression equation for fetal liver elasticity values with respect to GW is provided below:

$$E_{liver}(\text{Unit:kPa}) = 1.743 + 0.1859GW - 0.002455GW^2 \left(R^2 = 0.37\right) \quad [2]$$

The cubic regression equation representing the fetal lung-liver elasticity (LLE) ratio in relation to GW is as follows:

$$E_{LLE}(\text{Unit:kPa}) = -1.825 + 0.2651GW - 0.008392GW^2 + 8.550e-005GW^3 \left(R^2 = 0.14\right) \quad [3]$$

Table 2 Fetal lung and liver elasticity values and LLE ratio at different gestational weeks

Weeks of gestation	Pulmonary elasticity value (kPa)	Liver elasticity value (kPa)	LLE ratio	Weeks of gestation	Pulmonary elasticity value (kPa)	Liver elasticity value (kPa)	LLE ratio
20	3.68±0.30	4.52±0.31	0.82±0.06	30	4.58±0.27	5.16±0.41	0.89±0.06
21	3.70±0.35	4.68±0.29	0.79±0.07	31	4.58±0.26	5.21±0.40	0.88±0.08
22	4.00±0.30	4.55±0.33	0.88±0.09	32	4.48±0.26	5.18±0.28	0.87±0.07
23	4.21±0.30	4.71±0.36	0.90±0.08	33	4.47±0.27	5.22±0.28	0.86±0.06
24	4.22±0.37	4.79±0.31	0.88±0.08	34	4.44±0.29	5.24±0.26	0.85±0.08
25	4.20±0.21	4.82±0.32	0.87±0.07	35	4.35±0.45	5.31±0.34	0.82±0.08
26	4.30±0.26	4.78±0.35	0.90±0.08	36	4.39±0.21	5.24±0.32	0.84±0.07
27	4.40±0.32	4.88±0.34	0.90±0.09	37	4.31±0.14	5.22±0.36	0.83±0.06
28	4.43±0.30	5.09±0.35	0.87±0.06	38	4.29±0.28	5.24±0.40	0.83±0.09
29	4.57±0.19	5.09±0.30	0.90±0.08	39	4.29±0.29	5.25±0.28	0.82±0.08

Quantitative variables are expressed as mean ± standard deviation. LLE ratio, lung-to-liver elasticity ratio.

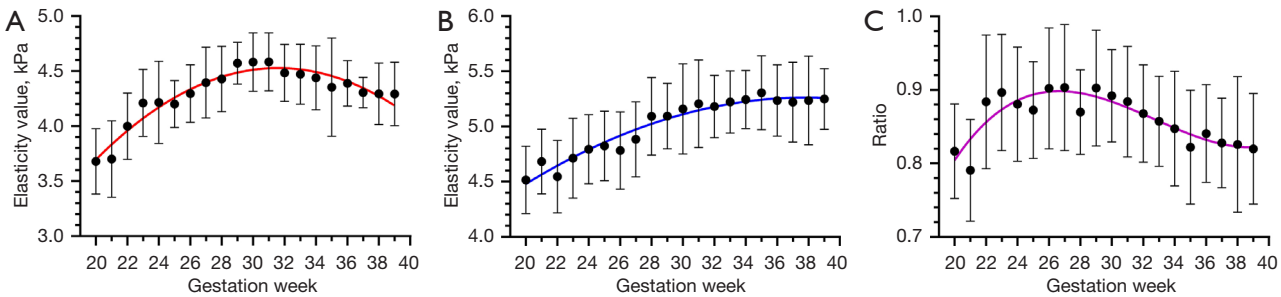

Figure 4 Curves of fetal lung and liver elasticity values and lung-to-liver elasticity ratio with gestational week. (A-C) The fitted curves of fetal pulmonary elasticity values (red curve), hepatic elasticity values (blue curve), and lung-to-liver elasticity ratio (purple curve) at different gestational weeks.

Measurements related to the fetus to be induced and observation of lung tissue sections after induction of labor

Table 3 provides details on the induced fetuses. It is noteworthy that one of the induced fetuses exhibited diminished normal lung tissue due to a large cystic adenoma of the lung, which hindered the observation of lung development stages through the available sections. The results of the study indicated that among the induced fetuses, a total of five cases (5/14, 35.7%) showed microscopic lung histology at an earlier stage of development compared to their ultrasound-determined gestational age, suggesting delayed fetal lung development. These cases included one instance of chromosome 1 deletion, one case of chromosome 2 deletion, one case of right heart dysplasia syndrome, one case of Tetralogy of Fallot combined with the absence of the right kidney, and one case of cystic occupancy in the adrenal gland area. Additionally, there was one case of anal atresia where the microscopic lung histology stage exceeded the ultrasound-determined gestational age stage.

The findings of the current study indicated that the predicted lung developmental stages based on fetal lung elasticity values showed a 71.4% agreement with microscopic lung histologic stages. Children with Lowe syndrome and cleft lip exhibited lower lung elasticity values than normal values at their corresponding lung development stage, while children with bilateral cleft lip and palate and tetralogy of Fallot combined with the absence of the right kidney displayed higher lung elasticity values than normal values at their respective lung development stages. *Figure 5* illustrates sections

Table 3 Basic information and measured values of induced fetuses

No.	Maternal age (years)	Pulmonary elasticity value (kPa)	Liver elasticity value (kPa)	LLE ratio	Ultrasound gestational age (weeks) (corresponding stage of lung development)	Microscopic lung histologic stage (degree of lung development)	Stages of lung development predicted from lung elasticity values	Consistency	Main reasons for induced abortion
1	35	3.48	4.63	0.75	25 (C+D)	C (delay)	C	O	Chromosome 1 deletion
2	35	3.54	4.11	0.86	23 (C)	C (normal)	C	O	Spina bifida
3	32	3.79	4.64	0.82	24 (C+D)	C+D (normal)	C	X	Lowe syndrome
4	34	4.12	4.39	0.94	24 (C+D)	C (delay)	C	O	Hypoplastic right heart syndrome
5	20	4.40	4.93	0.89	29 (D)	D (normal)	D	O	Absent nasal bone
6	30	4.24	4.94	0.86	26 (C+D)	C+D (normal)	C+D	O	Aberrant right subclavian artery combined with arrhythmia
7	35	3.91	4.24	0.92	37 (D+E)	E (overdue)	E	O	Anal atresia
8	22	3.88	4.58	0.85	32 (D)	C (delay)	C	O	Cystic occupations in the adrenal region
9	21	4.29	4.60	0.93	23 (C)	C (normal)	C+D	X	Bilateral cleft lip and palate
10	29	3.45	4.14	0.83	21 (C)	C (normal)	C	O	Trisomy 21
11	25	3.48	4.21	0.83	22 (C)	C (normal)	C	O	Unknown
12	36	4.26	5.12	0.83	23 (C)	–	C+D	–	Giant cystadenoma of the lungs
13	34	3.70	4.20	0.88	21 (C)	B+C (delay)	C	X	Tetralogy of Fallot combined with absence of the right kidney
14	19	4.00	4.44	0.90	25 (C+D)	C+D (normal)	C	X	Cleft lip
15	26	4.05	4.66	0.87	31 (D)	C (delay)	C	O	Chromosome 2 deletion

+, indicates a transitional stage between two lung developmental stages; –, non-judgmental. LLE ratio, lung-to-liver elasticity ratio; B, the pseudoglandular stage; C, the canalicular stage; D, the saccular stage; E, the alveolarization; O, lung elasticity value staging is concordant with microscopic lung tissue staging; X, lung elasticity value staging is discordant with microscopic lung tissue staging.

of fetal lung tissue following partial induction of labor.

Discussion

The current study's findings indicate that fetal pulmonary elasticity values tend to increase initially and then decrease during the second and third trimesters. In contrast, hepatic elasticity values consistently increase throughout pregnancy, although the rate of increase decelerates progressively. This pattern mirrors the results reported by Nallet *et al.* (15),

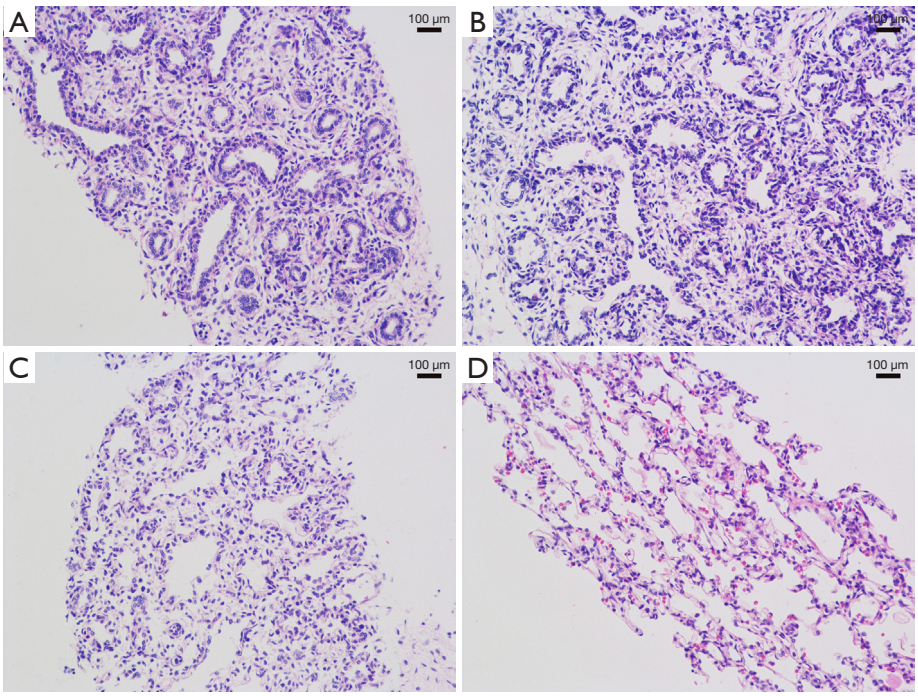

Figure 5 Hematoxylin-eosin stained sections of fetal lung tissue after induction of labor (×200). (A) Section of lung tissue at the transition between the pseudoglandular stage and the canalicular stage, taken from a fetus at 21 weeks of gestation, induced for tetralogy of Fallot combined with right renal agenesis and pulmonary developmental delay; (B) section of lung tissue at the canalicular stage, taken from a fetus at 23 weeks gestation, induced for spina bifida; (C) section of lung tissue at the transition between the canalicular stage and the saccular stage, taken from a fetus at 25 weeks of gestation, induced for cleft lip; (D) section of lung tissue in the alveolarization, taken from a fetus at 37-week gestation, induced for anal atresia.

with notable distinctions. Firstly, our study included a different normal fetus at each GW, whereas Nallet *et al.* assessed the same fetus across different GW. Secondly, Nallet *et al.*'s findings indicated that liver elasticity values were lower than lung elasticity values at the same GW until 36 GW. Conversely, our results demonstrated that liver elasticity values consistently exceeded lung elasticity values at the same GW within the 20–39 GW range. Fetal liver development is modulated by blood flow from the portal vein, hepatic artery, and umbilical vein. The influence of the portal vein on fetal hepatic blood flow diminishes with advancing GW (16). Additionally, transforming growth factor secreted by the portal mesenchyme plays a crucial role in promoting the differentiation of hepatocytes and cholangiocytes (17). Consequently, hepatocyte and cholangiocyte differentiation decelerates in the later stages of gestation, explaining the continuous increase in fetal liver elasticity values throughout pregnancy and the deceleration of the prenatal increase. Paruszewska-Achtel *et al.*'s study (18) demonstrated a logarithmic increase in liver morphometric parameters without gender differences, a trend that parallels to our fetal liver elastometry results. In contrast, Tongprasert *et al.*'s study (19) indicated a linear increase in liver morphologic parameters with GW. Minor discrepancies between the two studies may stem from variations in measurement methods and potential measurement errors. The work of da Silva *et al.* (12), utilizing the acoustic radiation force impulse (ARFI) strain imaging technique to measure pulmonary and hepatic elasticity values in sheep fetuses of normal pregnancy, is consistent with the trends observed in the present study. The LLE ratio is often used to compare two tissues using the liver as the reference organ (13,14) or to compare normal fetuses with those exhibiting fetal lung and liver alterations due to certain diseases (20). The present study revealed that the LLE ratio exhibited an initial increase followed by a decrease, with a gradual deceleration in the rate of decrease in the later stages. However, this finding slightly differs from previous results (13,19). In our previous study, we found that the fetal LLE ratio was

approximately 0.87 before 30 GW. In contrast, the study by Mottet *et al.* (20). reported that the fetal LLE ratio from 24 to 34 weeks of gestation remained constant at a mean value of 0.6. While both studies observed similar trends, the ratios differed, as did the trends compared to the present study. This discrepancy may be attributed to the nature of our previous longitudinal study, which averaged measurements within specific GW ranges. In contrast, the current study employed a cross-sectional approach, calculating measurements individually for each week of gestation, resulting in slightly different outcomes. Establishing reference ranges for the elasticity values of fetal lungs and liver, as well as the LLE ratio, based on these findings will aid in the noninvasive assessment of fetal lung and liver development. Moreover, it will simplify the use of the LLE ratio to evaluate the impact of various diseases on fetal lung and liver development, such as congenital diaphragmatic hernia and biliary atresia.

Morphologic changes in fetal lung development with advancing GW closely mirrored the findings of Drozdowska *et al.* (21). During the canalicular stage, no new airways are formed compared to the pseudoglandular stage; however, the interstitial cells increase in number and density. During the saccular stage, the distal portion of the airway undergoes separation and progressively elongates and widens, forming a balloon-like structure. In the alveolarization stage, the respiratory epithelium of alveoli comprises a single layer of cells. Our study identified fetal lung developmental delay in fetuses with deletions of chromosomes 1 and 2, hypoplastic right heart syndrome, tetralogy of Fallot combined with the absence of the right kidney, and cystic occupancies in the adrenal region. Previous studies have suggested global developmental delay in fetuses with chromosome 1 or chromosome 2 deletions (22-24); however, conclusive evidence linking this to pulmonary developmental delay is lacking. Fetuses with congenital heart diseases, such as hypoplastic right heart syndrome and tetralogy of Fallot, may suffer from right heart dysfunction due to structural abnormalities of the heart. Consequently, this affects pulmonary vascular development, leading to delayed lung development (25-27). In clinical practice, corticosteroids are commonly used to enhance fetal lung maturation (28,29). Adrenal region occupancy may affect the synthesis and release of adrenocorticotropic hormones, potentially delaying fetal lung development. Additionally, the present study documented a case of anal atresia in which the development stage of microscopic lung histology diverged from the ultrasound-determined gestational age. Research suggests that fetal anal atresia in early pregnancy causes transient intestinal dilatation (30-32). This dilatation increases pressure in the intestinal lumen, leading to elevated abdominal cavity pressure (33). Consequently, diaphragm elevation compresses the thoracic cavity. However, there is no definitive theoretical support indicating whether the cascade effect triggered by anal atresia can indeed impact fetal lung development.

The compliance rate between the predicted stages of fetal lung development based on fetal lung elasticity values and microscopic observations was 71.4%. This suggests that the 2D-SWE technique can be partially utilized to aid in assessing various developmental stages of the fetal lung. However, for greater accuracy, combining this technique with other examination methods is advisable. Discrepancies between the stages of lung development, classified in this study based on lung elasticity values and microscopic observations, were evident in fetuses with Lowe syndrome, bilateral cleft lip and palate, cleft lip, and tetralogy of Fallot combined with right renal absence. Research has demonstrated that elastometric values of various organs are associated with the obstruction of perfusion and drainage channels, as well as the structure and type of tissue (34,35). Changes in fetal pulmonary elasticity values may be attributed to reduced pulmonary blood flow and increased pulmonary artery pressure due to pulmonary artery stenosis in fetuses with tetralogy of Fallot. Amniotic fluid, primarily derived from urine secretion and fetal lungs, is mainly expelled through fetal swallowing. The circulation of amniotic fluid through fetal swallowing is crucial for lung development (36). Conversely, Toscano *et al.* (37) demonstrated that fetuses with cleft lip and palate had a significantly smaller gastric vesicle size compared to normal gestational fetuses, suggesting impairment in amniotic fluid swallowing. Consequently, obstruction of amniotic fluid circulation due to swallowing issues in fetuses with cleft lip and palate may affect fetal pulmonary elastometry to some extent. Further research is needed to investigate whether Lowe syndrome can affect the stiffness of fetal lung tissue.

There are some limitations in this study. All included pregnant women were of Asian ethnicity, potentially limiting the generalizability of the findings to other populations. Furthermore, our findings regarding the concordance between the stage of fetal lung development predicted using 2D-SWE and the stage of lung development observed microscopically were derived from induced fetuses with major malformations, thus making it challenging to generalize these results to normal

fetuses. In addition, cultural factors contributed to most mothers' reluctance to consent to fetal autopsy after induced abortion, resulting in a limited number of post-induced fetal lung tissues available. Further validation of the findings of this study is crucial through larger clinical trials with increased sample sizes.

Conclusions

Fetal lung and liver elasticity values, along with the LLE ratio, demonstrated distinct patterns across GW. The study found a 71.4% agreement between the fetal lung development stages predicted by lung elasticity values and those determined through histological analysis of lung tissue sections. Therefore, 2D-SWE emerges as a valuable tool for assessing fetal lung development and potentially guiding clinical decisions regarding drug administration to enhance lung maturation.

Acknowledgments

This article was linguistically edited by chatGPT.
Funding: None.

Footnote

Reporting Checklist: The authors have completed the STROBE reporting checklist. Available at https://qims.amegroups.com/article/view/10.21037/qims-24-272/rc

Conflicts of Interest: All authors have completed the ICMJE uniform disclosure form (available at https://qims.amegroups.com/article/view/10.21037/qims-24-272/coif). The authors have no conflicts of interest to declare.

Ethical Statement: The authors are accountable for all aspects of the work in ensuring that questions related to the accuracy or integrity of any part of the work are appropriately investigated and resolved. The study adhered to the Declaration of Helsinki (revised in 2013). It was approved by the institutional review board of the Second Affiliated Hospital of Fujian Medical University (No. 2022296) and registered at chictr.org.cn (ChiCTR2300077320). Quanzhou Women's and Children's Hospital was also informed and agreed to participate in the study. All pregnant women involved provided informed consent by signing a consent form.

References

1. Schittny JC. Development of the lung. Cell Tissue Res 2017;367:427-44.
2. Carraro S, Filippone M, Da Dalt L, Ferraro V, Maretti M, Bressan S, El Mazloum D, Baraldi E. Bronchopulmonary dysplasia: the earliest and perhaps the longest lasting obstructive lung disease in humans. Early Hum Dev 2013;89 Suppl 3:S3-5.
3. Butler JP, Loring SH, Patz S, Tsuda A, Yablonskiy DA, Mentzer SJ. Evidence for adult lung growth in humans. N Engl J Med 2012;367:244-7.
4. Rezaie Keikhaie K, Kahkhaie KR, Mohammadi N, Amjadi N, Forg AA, Ramazani AA. Relationship between Ultrasonic Marker of Fetal Lung Maturity and Lamellar Body Count. J Natl Med Assoc 2017;109:294-8.
5. Tang Y, Jin XD, Xu L, Deng Y, Chang Z, Li Q, Peng XL. The Value of Ultrasonography in Assessing Fetal Lung Maturity. J Comput Assist Tomogr 2020;44:328-33.
6. Khalifa YEA, Aboulghar MM, Hamed ST, Tomerak RH, Asfour AM, Kamal EF. Prenatal prediction of respiratory distress syndrome by multimodality approach using 3D lung ultrasound, lung-to-liver intensity ratio tissue histogram and pulmonary artery Doppler assessment of fetal lung maturity. Br J Radiol 2021;94:20210577.
7. Cui XW, Li KN, Yi AJ, Wang B, Wei Q, Wu GG, Dietrich CF. Ultrasound elastography. Endosc Ultrasound 2022;11:252-74.
8. Balleyguier C, Ciolovan L, Ammari S, Canale S, Sethom S, Al Rouhbane R, Vielh P, Dromain C. Breast elastography: the technical process and its applications. Diagn Interv Imaging 2013;94:503-13.
9. Monpeyssen H, Tramalloni J, Poirée S, Hélénon O, Correas JM. Elastography of the thyroid. Diagn Interv Imaging 2013;94:535-44.
10. Dudea SM, Giurgiu CR, Dumitriu D, Chiorean A, Ciurea A, Botar-Jid C, Coman I. Value of ultrasound elastography

in the diagnosis and management of prostate carcinoma. Med Ultrason 2011;13:45-53.
11. Gheonea DI, Săftoiu A, Ciurea T, Gorunescu F, Iordache S, Popescu GL, Belciug S, Gorunescu M, Săndulescu L. Real-time sono-elastography in the diagnosis of diffuse liver diseases. World J Gastroenterol 2010;16:1720-6.
12. da Silva PDA, Uscategui RAR, Santos VJC, Taira AR, Mariano RSG, Rodrigues MGK, Simões APR, Maronezi MC, Avante ML, Monteiro FOB, Vicente WRR, Feliciano MAR. Acoustic radiation force impulse (ARFI) elastography to asses maternal and foetal structures in pregnant ewes. Reprod Domest Anim 2019;54:498-505.
13. Mottet N, Aubry S, Vidal C, Boiteux G, Metz JP, Riethmuller D, Pazart L, Ramanah R. Feasibility of 2-D ultrasound shear wave elastography of fetal lungs in case of threatened preterm labour: a study protocol. BMJ Open 2017;7:e018130.
14. Mottet N, Cochet C, Vidal C, Metz JP, Aubry S, Bourtembourg A, Eckman-Lacroix A, Riethmuller D, Pazart L, Ramanah R. Feasibility of two-dimensional ultrasound shear wave elastography of human fetal lungs and liver: A pilot study. Diagn Interv Imaging 2020;101:69-78.
15. Nallet C, Pazart L, Cochet C, Vidal C, Metz JP, Jacquet E, Gorincour G, Mottet N. Prenatal quantification of human foetal lung and liver elasticities between 24 and 39 weeks of gestation using 2D shear wave elastography. Eur Radiol 2022;32:5559-67.
16. Kruepunga N, Hakvoort TBM, Hikspoors JPJM, Köhler SE, Lamers WH. Anatomy of rodent and human livers: What are the differences? Biochim Biophys Acta Mol Basis Dis 2019;1865:869-78.
17. Trefts E, Gannon M, Wasserman DH. The liver. Curr Biol 2017;27:R1147-51.
18. Paruszewska-Achtel M, Dombek M, Badura M, Elminowska-Wenda GM, Wiśniewski M, Szpinda M. Quantitative anatomy of the liver visceral surface in the human fetus. Adv Clin Exp Med 2018;27:1131-9.
19. Tongprasert F, Srisupundit K, Luewan S, Tongsong T. Normal length of the fetal liver from 14 to 40 weeks of gestational age. J Clin Ultrasound 2011;39:74-7.
20. Mottet N, Metz JP, Chaussy Y. Evolution of fetal lung stiffness during gestation in two different congenital malformations. J Obstet Gynaecol Res 2019;45:931-4.
21. Drozdowska J, Cousens C, Finlayson J, Collie D, Dagleish MP. Structural Development, Cellular Differentiation and Proliferation of the Respiratory Epithelium in the Bovine Fetal Lung. J Comp Pathol 2016;154:42-56.
22. Tim-Aroon T, Jinawath N, Thammachote W, Sinpitak P, Limrungsikul A, Khongkhatithum C, Wattanasirichaigoon D. 1q21.3 deletion involving GATAD2B: An emerging recurrent microdeletion syndrome. Am J Med Genet A 2017;173:766-70.
23. Bloch M, Leonard A, Diplas AA, Pepermans X, Emanuel BS, Santa Rocca M, Revencu N, Sznajer Y. Further phenotype description, genotype characterization in patients with de novo interstitial deletion on 2p23.2-24.1. Am J Med Genet A 2014;164A:1789-94.
24. Liang JS, Shimojima K, Ohno K, Sugiura C, Une Y, Ohno K, Yamamoto T. A newly recognised microdeletion syndrome of 2p15-16.1 manifesting moderate developmental delay, autistic behaviour, short stature, microcephaly, and dysmorphic features: a new patient with 3.2 Mb deletion. J Med Genet 2009;46:645-7.
25. Guo Y, Liu X, Gu X, Zhang Y, Sun L, He Y. Fetal lung volume and pulmonary artery changes in congenital heart disease with decreased pulmonary blood flow: Quantitative ultrasound analysis. Echocardiography 2018;35:85-9.
26. Guerin S, Bertille N, Khraiche D, Bonnet D, Lebourgeois M, Goffinet F, Lelong N, Khoshnood B, Delacourt C; EPICARD study group. Respiratory morbidity in children with congenital heart disease. Arch Pediatr 2021;28:525-9.
27. Ruchonnet-Metrailler I, Bessieres B, Bonnet D, Vibhushan S, Delacourt C. Pulmonary hypoplasia associated with congenital heart diseases: a fetal study. PLoS One 2014;9:e93557.
28. Williams MJ, Ramson JA, Brownfoot FC. Different corticosteroids and regimens for accelerating fetal lung maturation for babies at risk of preterm birth. Cochrane Database Syst Rev 2022;8:CD006764.
29. D'Souza R, Ashraf R, Rowe H, Zipursky J, Clarfield L, Maxwell C, Arzola C, Lapinsky S, Paquette K, Murthy S, Cheng MP, Malhamé I. Pregnancy and COVID-19: pharmacologic considerations. Ultrasound Obstet Gynecol 2021;57:195-203.
30. Taipale P, Rovamo L, Hiilesmaa V. First-trimester diagnosis of imperforate anus. Ultrasound Obstet Gynecol 2005;25:187-8.
31. Lam YH, Shek T, Tang MH. Sonographic features of anal atresia at 12 weeks. Ultrasound Obstet Gynecol 2002;19:523-4.
32. Kaponis A, Paschopoulos M, Paraskevaidis E, Makrydimas G. Fetal anal atresia presenting as transient bowel dilatation at 16 weeks of gestation. Fetal Diagn Ther 2006;21:383-5.
33. Madl C, Druml W. Gastrointestinal disorders of the

critically ill. Systemic consequences of ileus. Best Pract Res Clin Gastroenterol 2003;17:445-56.
34. Habibi HA, Cicek RY, Kandemirli SG, Ure E, Ucar AK, Aslan M, Caliskan S, Adaletli I. Acoustic radiation force impulse (ARFI) elastography in the evaluation of renal parenchymal stiffness in patients with ureteropelvic junction obstruction. J Med Ultrason (2001) 2017;44:167-72.
35. Correas JM, Anglicheau D, Gennisson JL, Tanter M. Élastographie rénale. Nephrol Ther 2016;12:S25-S34.
36. Jha P, Raghu P, Kennedy AM, Sugi M, Morgan TA, Feldstein V, Põder L, Penna R. Assessment of Amniotic Fluid Volume in Pregnancy. Radiographics 2023;43:e220146.
37. Toscano M, Burhans K, Mack LM, Henderson S, Koltz PF, Girotto JA, Thornburg LL. Prenatal Ultrasound Measurement of Fetal Stomach Size Is Predictive of Postnatal Development of GERD in Isolated Cleft Lip and/or Palate. Cleft Palate Craniofac J 2021;58:881-7.

Cite this article as: Liu D, Jiang Q, Xu Z, Li L, Lyu G. Evaluating fetal lung development at various gestational weeks using two-dimensional shear wave elastography. Quant Imaging Med Surg 2024;14(8):5373-5384. doi: 10.21037/qims-24-272

